# CHAPTER 40

# Probabilistic Calculation Model of Directional Random Waves

Wi-Gwang Pae[1], Hajime Mase[2], M. ASCE
and Tetsuo Sakai[3], M. ASCE

**ABSTRACT:** A probabilistic calculation model is developed, for the simplicity of inclusion of wave breaking and energy dissipation, to predict the transformation of directionally-spreading random waves by using parabolic refraction-diffraction equations. The numerical predictions are compared with the experimental observations of random wave transformation over an elliptic shoal by Vincent and Briggs (1989); the predictions agree well with the observations under the non-breaking condition, however, the agreement is poor under the wave breaking condition.

## INTRODUCTION

Estimation of refraction and diffraction, shoaling and wave breaking deformation over complicated bathymetry is an important problem in coastal engineering. Although random sea state is usually approximated by a monochromatic wave equivalent to the significant wave, there are some differences between the actual sea state and the results of monochromatic representation.

There are mainly two methods to deal with transformations of random waves: that is, spectral and individual wave analysis methods. Here we employ the individual wave analysis method for the simplicity of inclusion of wave breaking and energy dissipation. Incident wave heights and incident angles of individual waves are given from probabilistic density functions of wave heights and angles, and periods are given depending on their wave heights. Model wave equations used here are two different parabolic refraction-diffraction equations depending on incident angles. The numerical predictions are compared with the experimental observations of wave transformations of directionally-spreading random waves over an elliptic shoal carried out by Vincent and Briggs (1989).

1) Consulting Engineer, Nikken Consultants, Inc., Shinagawa-Ku, Tokyo, 141, Japan.
2) Res. Assoc., and 3) Prof., Department of Civil Eng., Kyoto Univ., Kyoto, 606, Japan.

# NUMERICAL MODEL FOR DIRECTIONAL RANDOM WAVES

## Input Wave Heights

One-parameter Weibull distribution was adopted as an input wave height distribution (Mase and Kobayashi, 1991).

$$p(x) = \frac{m}{2\phi} h_{1/3}^{m} x^{m-1} \exp\left\{-\frac{1}{2\phi}(h_{1/3}\,x)^{m}\right\} , \tag{1}$$

$$h_{1/3} = \frac{3m}{2\phi} \int_{(2\phi \ln 3)^{1/m}}^{\infty} h^{m} \exp\left(-\frac{h^{m}}{2\phi}\right) dh , \tag{2}$$

$$\phi = \frac{1}{2}\left[\Gamma\left(\frac{m+1}{m}\right)\right]^{-m} , \tag{3}$$

where $x$ is the wave height normalized by the significant wave height, $H_0$, $\Gamma$ is the Gamma function, and $m$ is the shape factor related to the wave groupiness factor, $GF$, as described by

$$m = 3.44 - 1.99\,GF, \tag{4}$$

according to Mase (1989) and Mase et al. (1990). Therefore, the effect of wave grouping is indirectly taken into account in the wave transformation model through Eq.(4).

From the Weibull distribution, representative individual wave heights were defined by dividing $x$, ranging from 0 to 2, into $N$ (=20) segments, $x_i$ ($i = 1,..., N$), and the corresponding occurrence probabilities, $p_i$ ($i = 1,...,N$) were calculated. A dimensional wave height is given by $x_i * H_0$.

## Input Wave Periods

Considering that higher waves have longer periods and referring observed joint distributions of wave heights and periods (Goda, 1978), we set wave periods as

$$\left.\begin{array}{ll} T_i = 0.6\,T_0 ; & 0 < H_i \leq 0.5H_0 , \\ T_i = T_0 ; & 0.5H_0 < H_i \leq 1.5H_0 , \\ T_i = 1.2\,T_0 ; & 1.5H_0 < H_i , \end{array}\right\} \tag{5}$$

in a simple manner, where $T_0$ is the significant wave period.

An alternative way to give input wave heights and periods is to use a joint probability density function of wave heights and periods; however, this method results in more number of waves in the calculation of wave transformation than the present method, since several wave periods are defined for a given wave height.

## Input Incident Wave Angles

Here directional spreading of individual waves was considered as in the case of spectral method (Panchang et al., 1990). Directional distributions of individual waves were assumed to be described by the following function:

$$G(\theta) = G_0 \cos^{2S}\{(\theta - \theta_0)/2\} , \qquad (6)$$

where $\theta_0$ is the principal (mean) direction against the $x$ axis, $S$ is the parameter representing the degree of directional concentration , $G_0$ is the constant to make the integration of Eq.(6) unity. Eq.(6) was originally proposed for spectral components (Mitsuyasu et al., 1975); which was treated as a probability density function of incident angles here.

Assuming that the directional distribution of individual waves is narrow compared to that of spectral components, and since parabolic refraction-diffraction equations are employed as model wave equations, we limit the maximum absolute value of $\theta$ to 60°. The representative incident wave angles, $\theta_j$ ($j = 1, ..., M$), were given by every 10° in the range between - 60° and 60°, and the corresponding occurrence probabilities, $q_j$ ($j = 1, ..., M$), were determined from Eq.(6).

The directional spreading function used by Vincent and Briggs (1989) was

$$G(\theta) = \frac{1}{2\pi} + \frac{1}{\pi} \sum_{j=1}^{J} \exp\left\{ -\frac{(j\sigma)^2}{2} \right\} \cos j(\theta - \theta_0) . \qquad (7)$$
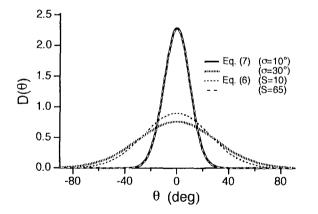


Fig. 1  Comparison of directional spreading functions.

If $S$ in Eq.(6) is assigned to 400, 65, or 10, the directional distribution by Eq.(6) corresponds to that by Eq.(7) with $\sigma = 0°$, $10°$ or $30°$, used as the experimental conditions of uni-directional, narrow-, or broad-banded directional spreading by Vincent and Briggs (1989). Figure 1 shows the comparison of the two directional distributions by Eqs.(6) and (7). It is seen from the figure that both almost agree.

**Model Wave Equation**

Transformations of all $N*M$ individual waves of wave heights $H_i$, wave periods $T_i$, and incident angles $\theta_j$, with the occurrence probabilities $p_i*q_j$, were calculated by parabolic refraction-diffraction equations. The calculated results were superposed according to their occurrence probabilities. For waves with large incident angle $|\theta_j| \geq 5°$, the minimax approximation model of Kirby (1986) was used:

$$A_x + i\ (\bar{k}-a_0 k)A + \frac{C_{gx}}{2C_g}A + \frac{i}{\omega C_g}\left(a_1 - b_1\frac{\bar{k}}{k}\right)(CC_g A_y)_y - \frac{b_1}{\omega k C_g}(CC_g A_y)_{yx}$$
$$+ \frac{b_1}{\omega}\left(\frac{k_x}{k^2 C_g} + \frac{C_{gx}}{2kC_g^2}\right)(CC_g A_y)_y - \left(a_1 - b_1\frac{\bar{k}}{k}\right)\frac{W}{C_g}A$$
$$+ i\ b_1\left(\frac{k_x}{kC} + \frac{C_{gx}}{2kC_g^2}\right)WA - \frac{ib_1}{kC_g^2}W_x A - \frac{ib_1}{kC_g^2}WA_x = 0 \ , \tag{8}$$

where $A$ is the complex amplitude, $\bar{k}$ is the wave number averaged over the $y$ direction, $k$ is the local wave number, $C_g$ is the group velocity, $\omega$ is the angular frequency, $W$ is the damping coefficient described later, and $a_0$, $a_1$, $b_1$ are the coefficients taken to be 0.9947, -0.8900, -0.4516. It is noted that the derivative of $W$ was included in Eq.(8) compared to the original minimax model of Kirby (1986).

For waves with small incident angle $|\theta_j| < 5°$, the following parabolic equation with an energy dissipation term was used:

$$A_x - i\ (K - \overline{k_0})A + \frac{(KCC_g)_x}{2KCC_g}A - \frac{i}{2KCC_g}(CC_g A_y)_y = 0 \ , \tag{9}$$

$$K^2 = k^2 + i\ \frac{kW}{C_g} \ , \tag{10}$$

where $\overline{k_0}$ is the wave number at the incident boundary averaged over the $y$ direction. Eq.(9) is obtained from the mild slope equation with a damping term (Booij, 1981) by using the splitting matrix method (Radder, 1979; Dalrymple et al., 1984).

Incipient of wave breaking was estimated by a simple equation,

$$H_b / h_b = 0.85 (0.7 + 5 \tan\beta ) \ , \tag{11}$$

where $H_b$ and $h_b$ are the wave height and depth at the breaking point, $\tan\beta$ is the bottom slope.

The damping coefficient in Eqs.(8) and (10) was formulated by a bore model (Battjes, 1986) as follows:

$$W = \frac{2B}{\gamma^3} \frac{1}{T} \left(\frac{H}{h}\right)^4 , \tag{12}$$

$$\gamma = 0.7 + 5 \tan\beta , \tag{13}$$

$$B = \begin{cases} 11\text{-}10 \, h/h_b , & 0.6 \le h/h_b \le 1.0 \\ 5, & h/h_b \le 0.6 . \end{cases} \tag{14}$$

Eq.(14) was used to represent the measured wave height change of monochromatic waves more accurate (Mase and Iwagaki, 1982). In the calculation, a treatment of the lateral boundary condition followed Yamamoto (1987).

## COMPARISON BETWEEN NUMERICAL PREDICTIONS AND EXPERIMENTAL OBSERVATIONS

Experiments of random wave transformations over a shoal were carried out by Vincent and Briggs (1989). Figure 2 illustrates the experimental layout of an elliptical shoal and measurement locations, but
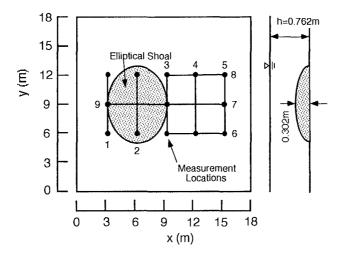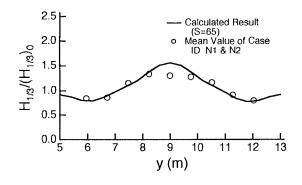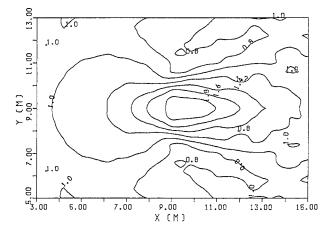


Fig. 2  Experimental layout.

the coordinates are rewritten so that the center of the shoal is located at $(x, y) = (6m, 9m)$, for the convenience in the numerical calculations. The TMA spectrum was used as a target spectrum. Spectral peakedness was changed by two; that is, broad-banded and narrow-banded frequency spectra. In the present model, an energy spectrum was not given as input data, but given by a wave height distribution. As general, a narrow-banded spectral wave trains lead to the Rayleigh distribution of wave heights.



(a)



(b)

**Fig. 3  Spatial wave height distribution for narrow-banded
directional spreading waves of Case N1 and N2.**

Figure 3 shows the comparison of measured and calculated wave heights along the measuring line #4 (figure (a)), and in a horizontal region (figure (b)), for the case of narrow-banded directional spreading waves with two different spectral peakedness of Case N1 and Case N2 in the paper of Vincent and Briggs (1989). Since the experimental results of N1 and N2 were almost the same, the experimental results were averaged and shown in Fig.3. In the calculation, the Rayleigh distribution ($m = 2$ in Eq.(1)) was given as the input wave height distribution. Comparing wave heights along the measuring line #4, we see a fairly good agreement between both results, but the calculated wave heights around $y = 9m$ are a little larger than the measured ones. One of the reasons of the discrepancy may be attributed to unsatisfactory smoothing due to inadequate number of division in both wave periods and incident angles in the calculation.

Figure 4 shows the comparison of wave heights along the measuring line #4 for the case of uni-directional random waves under the condition of non-breaking. In this figure, not only the significant wave height but also the one-hundredth maximum, the one-tenth maximum and the mean wave heights are plotted. Easiness to calculate such wave heights is one of the advantages of the present calculation method compared to spectral calculation methods. Experimental results of U3 and U4 were averaged in the figure. We can see a good agreement in this condition.
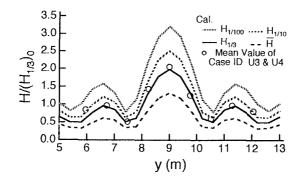


**Fig. 4 Comparison of measured and calculated wave heights along the measuring line #4 for uni-directional random waves.**

Figure 5 is the result of narrow-banded directional spreading waves of Case N3 and Case N4. Numerical predictions agree well with the observations.

Figure 6 shows the comparison for the case of broad-banded directional spreading random waves. The spatial wave height distribution along the measuring line #4 is very flat due to wide directional spreading. Averaged measured wave heights and calculated ones agree well. The
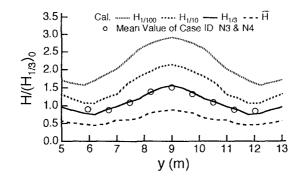
**Fig. 5** **Comparison of measured and calculated wave heights along the measuring line #4 for narrow-banded directional spreading random waves.**
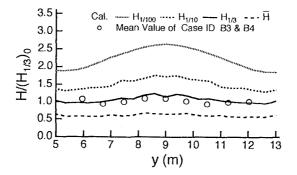


**Fig. 6** **Comparison of measured and calculated wave heights along the measuring line #4 for broad-banded directional spreading random waves.**

difference between the calculated one-hundredth and the mean wave heights around $y = 9$ m is larger than that in both sides; that is, the wave height distribution around $y = 9$ m becomes wider than that in both sides.

Figure 7 shows the effect of the shape factor of the Weibull distribution on the calculated wave heights along the measuring line #4. There is little difference in the significant wave heights, but we can see the difference for higher waves such as the one-hundredth maximum wave height. As the shape factor $m$ becomes small, that is, the incident wave height distribution becomes wider, the one-hundredth maximum wave height becomes large especially around $y = 9$ m.
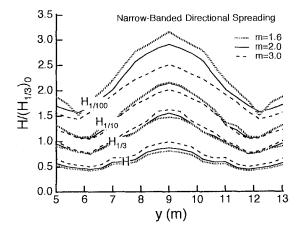
**Fig. 7  Effect of incident wave height distribution on calculated wave heights along measuring line #4.**
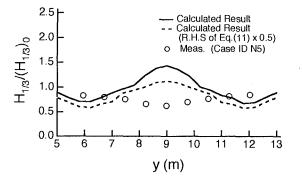


**Fig. 8  Comparison of measured and calculated wave heights under the wave breaking condition.**

Figure 8 shows a result of the cases that wave breaking occurred over the shoal. The measured spatial wave height distributions along the measuring line #4 are different from the calculated ones. The observations become minimum around $y = 9$ m, but the predictions are maximum. Even if the incipient condition of wave breaking was modified to make waves break at deeper water, by multiplying 0.5 to the original incipient condition, the shape of calculated spatial wave height distribution is unchanged, only resulting in smaller values (shown by broken line).

The following point should be noted. Experiments of uni-directional random wave transformations over a shoal were carried out by Lie and Tørum (1991). Even in the case that severe wave breaking occurred on the shoal, a concave wave height distribution along a transverse section, that is, being minimum of wave heights at the center of a transverse section cannot be seen, judging from contour maps of wave heights. The difference between the measured and the calculated wave heights under the wave breaking condition, and the difference between the measured results by different researchers may be attributed to the complexity of the breaking point and energy dissipation process over an arbitrary varying bathymetry.

## CONCLUSIONS

This study developed a probabilistic model to calculate transformations of directionally-spreading random waves, by using an incident wave height distribution, an incident angle distribution, and parabolic refraction-diffraction equations, for the simplicity of inclusion of wave breaking and energy dissipation. Other advantages of the present model were as follows: 1) the present model could estimate any representative wave heights including the significant wave height; and 2) could evaluate the effect of wave grouping through the relationship between the incident wave height distribution and groupiness factor. The experimental results of random wave transformations over an elliptic shoal by Vincent and Briggs (1989) agreed well with the predictions by the present numerical model in the case of non-breaking condition. In the case that wave breaking occurred on a shoal, the predictions were not in agreement with the observations. The shape of measured wave height distribution in a transverse section was concave, however, the calculated wave height distribution was convex. Therefore, one of the advantages of the present model, that is, the simplicity of inclusion of wave breaking process was not examined yet. The present model should be checked for other experimental observations over a shoal, since some of the observations showed a different pattern of wave height distribution.

## REFERENCES

Battjes, J.A. (1986). Energy dissipation in breaking solitary and periodic waves. Communications on Hydraulic and Geotech. Eng., Delft Univ. of Tech., Delft, 18p.

Booij, N. (1981). Gravity waves on water with non-uniform depth and current, Rep.81-1, Dept. of Civil Eng., Delft Univ. of Tech., Delft, 131p.

Dalrymple, R.A., Kirby, J.T. and Hwang, P.A. (1984). Wave diffraction due to areas of energy dissipation. Jour. Waterway, Port, Coastal, and Ocean Eng., Vol.110, No.1, pp.67-79.

Goda, Y. (1978). The observed joint distribution of periods and heights of sea waves. Proc. 16th Int. Conf. on Coastal Eng., ASCE, pp.227-246.

Kirby, J.T. (1986). Rational approximations in the parabolic equation method for water waves. Coastal Eng., Vol.10, No.4, pp.355-378.

Lie, V. and Tørum, A. (1991). Ocean waves over shoals. Coastal Eng., Vol.15, Nos.5&6, pp.545-562.

Mase, H. (1989). Groupiness factor and wave height distribution. Jour. Waterway, Port, Coastal, and Coastal Eng., ASCE, Vol.115, No.1, pp.105-121.

Mase, H. and Iwagaki, Y. (1982). Wave height distribution and wave grouping in surf zone. Proc. 18th Int. Conf. on Coastal Eng., ASCE, pp.58-76.

Mase, H., Hayashi, K. and Yamashita, T. (1990). Wave group properties of coastal waves. Proc. 22nd Int. Conf. on Coastal Eng., ASCE, pp.177-190.

Mase, H. and Kobayashi, N. (1991). Transformation of random breaking waves and its empirical numerical model considering surf beat. Proc. Coastal Sediments '91, ASCE, pp.688-702.

Mitsuyasu, H. et al. (1975). Observation of the directional spectrum of ocean waves using cloverleaf buoy, Jour. Physical Oceanogr., Vol.5, No.4, pp.750-760.

Panchang, V.G, Wei, G., Pearce, B.R. and Briggs, M.J. (1990). Numerical simulation of irregular wave propagation over shoal. Jour. Waterway, Port, Coastal, and Coastal Eng., ASCE, Vol.116, No.3, pp.324-340.

Radder, A.C. (1979). On the parabolic equation method for water-wave propagation. Jour. Fluid Mech., Vol.95, pp.159-176.

Vincent, C.L. and Briggs, M.J. (1989). Refraction-diffraction of irregular waves over a mound. Jour. Waterway, Port, Coastal, and Ocean Eng., ASCE, Vol.115, No.2, pp.269-284.

Yamamoto, A. (1987). Parabolic wave refraction-diffraction equation with dissipation and its applications. Master Thesis, Dept. of Civil Eng., Kyoto Univ., 103p.